

Dispersion and Transport of Energetic Particles due to the Interaction of Intense Laser Pulses with Overdense Plasmas

J. C. Adam, A. Héron, and G. Laval

Centre de physique Théorique, UMR7644, Ecole Polytechnique, 91128 Palaiseau, France

(Received 9 January 2006; published 17 November 2006)

We study the angular distribution of relativistic electrons generated through laser-plasma interaction with pulse intensity varying from 10^{18} W/cm² up to 10^{21} W/cm² and plasma density ranging from 10 times up to 160 times critical density with the help of 2D and 3D particle-in-cell simulations. This study gives clear evidence that the divergence of the beam is an intrinsic property of the interaction of a laser pulse with a sharp density gradient. It is entirely due to the excitation of large static magnetic fields in the layer of interaction. The energy deposited in this layer increases drastically the temperature of the plasma independently of the initial temperature. This makes the plasma locally collisionless and the simulation relevant for the current experiments.

DOI: [10.1103/PhysRevLett.97.205006](https://doi.org/10.1103/PhysRevLett.97.205006)

PACS numbers: 52.38.Fz, 52.35.Mw, 52.65.Rr

Many experiments now show that the interaction of an intense laser beam with a solid target yields a diverging beam of energetic particles with an angle ranging from 20° to 40° . Large open boundaries in both direction also show this effect contrary to the bunching observed in [1]. The magnetic field appears very early in time (typically on the 50 fs time scale) and starts to develop as very short wavelength filaments with wavelengths close to c/ω_p . As their amplitudes grow they tend to merge in somewhat larger wavelength filaments. Figure 1 is a blowup of the results of a simulation of the interaction of a Gaussian laser beam with a FWHM of 5μ and an intensity of 10^{20} W/cm² on an isolated plasma slab with a density of $80n_c$. The initial background electron temperature is 10 keV. The total size of the plasma slab is $285k_0^{-1} \times 400k_0^{-1}$ with $k_0 = 2\pi/\lambda$, where λ is the laser wavelength. The top figure shows, for particles with energy between 100 and 3000 keV, the mass current density extending from the layer of interaction ($\sim 200k_0^{-1}$) up to $320k_0^{-1}$ inside the plasma. This mass current density is superimposed on the structure of the low frequency magnetic field that is mostly concentrated in the interaction region where alternate red and blue short transverse scale filaments are visible. The presence of these filaments suggests the excitation of a Weibel-like instability. Their peak value is over 200 MG while inside the plasma the peak value of the magnetic fluctuations remains below 10 MG. The lower picture is a plot of the average rms value of the magnetic field at the same time (100 fs after the beginning of the interaction). It shows the extreme localization of the magnetic field with an average peak value of roughly 100 MG. This figure shows clearly that the divergence of particles occurs at the magnetic layer and the energetic particles then propagate freely inside the plasma. As mentioned in [2] the discrepancy with [1] is probably due to the size of the system. It agrees with the results of [3] that were obtained using an implicit model that describe the propagation of a beam of hot particles into

an overdense plasma. The object of this Letter is to demonstrate that the source of this divergence is indeed the magnetic layer that develops at the interface and also to study the effect of the dimensionality.

The problem with large 2D simulations is that they must be performed with a low resolution and a small number of particles per cell. Here we have chosen a small system and a very simple geometry in order to favor accuracy. The 2D and 3D systems use exactly the same geometry and mesh size. In order to keep the numerical noise as low as possible and to improve the statistic on the low density beam of

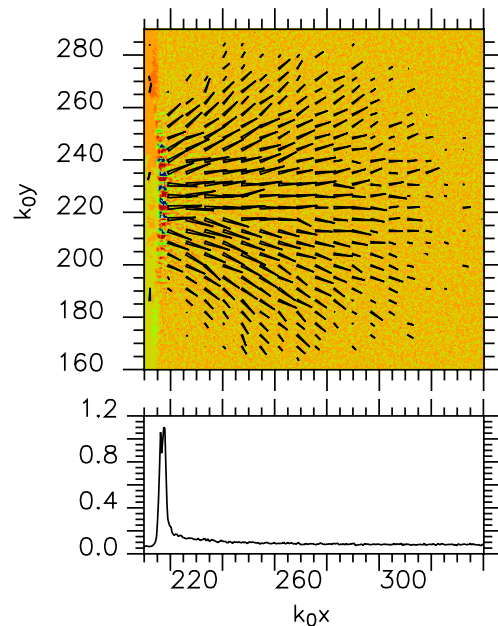


FIG. 1 (color online). (a) The mass flow of energetic particles ($W_{\text{cin}} > 100$ keV) superimposed on the structure of the magnetic field. (b) The rms value of the magnetic field calculated on the size of the focal spot.1 on the y scale corresponding to field amplitude of 100 MG.

energetic particles the number of particles per cell is 24 in 3D and 100 in 2D. The laser pulse propagates along the x direction and interacts with a plasma slab of a given density at normal incidence. The mesh size is $k_0 dy = k_0 dz = 0.1$ and $k_0 dx = 0.05$ in order to satisfy accuracy constraints. The simulation box has open-ended boundaries in the direction of propagation of the laser light and periodic boundary condition in the transverse direction(s). The plasma size is 2λ in the transverse direction(s) and approximately 65λ in the longitudinal one. There are approximately 16λ of vacuum on each side of the plasma slab. 2D simulations performed with a larger transverse direction yield the same results. The laser pulse has a flat time profile after a rising time of 25 fs. The irradiation is uniform in the transverse direction. The field is polarized linearly with the electric field along the y direction and the magnetic field in the z direction. The simulations were stopped at the time where the most energetic particles begin to reach the end of the box.

The preceding geometry is very close to the simulations that were performed in [4,5] but our work was mostly performed at higher density and intensity and on longer time scales. Our results basically agree with theirs. We see very rapidly magnetic filaments that develop at the edge of the plasma-vacuum interface on a thickness of the order of the skin depth c/ω_{pe} and an initial transverse wavelength of the same order of magnitude, as in global simulations. Similar structures have also been observed in [6,7]. The average profile of the low frequency magnetic field is very similar to the one in [3,4]. However we disagree with the statement [4] that 2D and 3D results differ significantly. The comparison of the magnetic field structure in 2D with cuts of the 3D structure reveals similar wavelengths and, as shown in Fig. 2, the longitudinal profiles of the low frequency magnetic fields are virtually identical. The initial

noise level depends both on the initial temperature (which is a physical effect) and the number of particles per cell (which for a plasma of given physical density is a numerical effect). The comparison of Fig. 2(a) and 2(b) shows clearly the effect of initial conditions on the development of the magnetic field. Both figures correspond to a plasma density of $80n_c$ and a flux of 10^{20} W/cm². Figure 2(a) corresponds to an initial temperature of 1 keV while Fig. 2(b) corresponds to an initial temperature of 10 keV, the solid line corresponds to the 2D case and the dashed line to the 3D one. This implies that there is a change in the anomalous resistivity as the background temperature of the plasma is decreased. For the present Letter the important point is that the structure of the boundary layer is independent of the initial temperature as well as of the number of particles. This independence is due to the fact that the electronic temperature in the layer increases as rapidly as the magnetic field and becomes very rapidly of the order of 100 keV, i.e., much larger than the initial temperature. The energy spectrum of particles in this layer is typically in the range from 100 keV up to 1 MeV. Starting with a colder temperature would merely add collisional absorption of the laser during a very short time and would not affect this result [3,8]. The differences between 2D and 3D results in mentioned in Ref. [4] come from the fact that the simulations [9] that were used as the basis of comparison were performed in a 2D geometry that did not allow a correct relaxation of the filamentation instability by forbidding the development of finite wave numbers along the direction of propagation of the energetic particles.

Figure 3 is a blowup of the electron phase space in the simulation corresponding to Fig. 2(a) 100 fs after the beginning of the interaction, close to saturation of the magnetic field growth. Figure 3(a) is the projection x, p_x where p_x is the longitudinal momentum. Bunches of energetic particles are clearly visible. The distance between them is $\lambda/2$, which implies an emission at frequency $2\omega_0$. This is the signature of the $J \times B$ mechanism of acceleration. Figures 3(b) and 3(c) are the transverse projections, respectively, (x, p_y) and (x, p_z) . Both projections show a spread of the transverse momentum, but the most distinctive feature is the apparition of 2 different kinds of bunches. In the direction of the laser electric field one can see bunched jets separated by half a vacuum wavelength corresponding to an emission at frequency $2\omega_0$, with a mean velocity oscillating at frequency ω_0 . This takes place immediately behind the surface of interaction and clearly reflects an interaction of the laser wave with energetic electrons within the skin depth, in the region of the magnetic layer. In the direction transverse to the electric field, one can also see bunched jets of electrons with an emission frequency which is again $2\omega_0$, without any mean velocity. These electron bunches are accelerated by the $J \times B$ mechanism and randomly deflected during their transport through the magnetic layer. 2D simulations performed

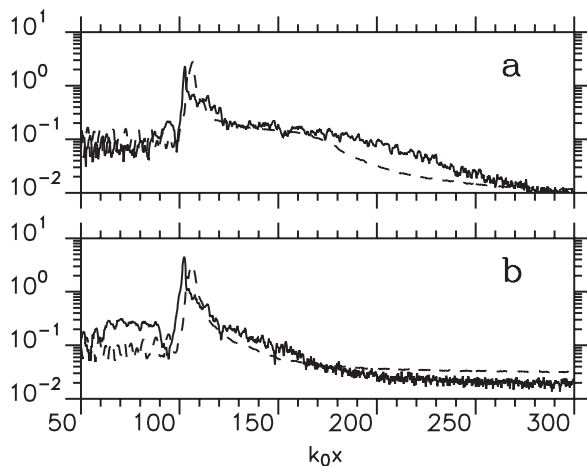


FIG. 2. Transverse average of the rms value of the low frequency magnetic field. (a) Initial electronic temperature 1 keV, (b) initial electronic temperature 10 keV. The solid line corresponds to the 2D simulation and the dashed line to the 3D one.

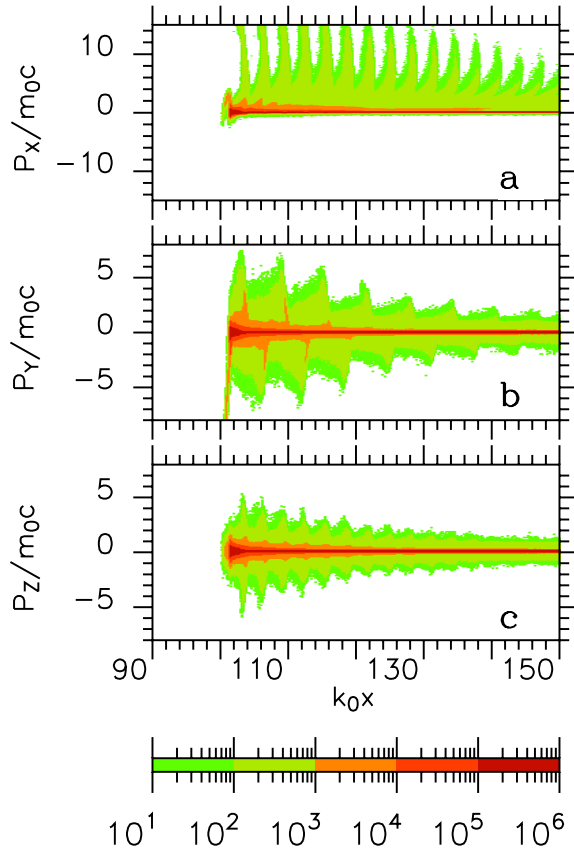


FIG. 3 (color online). Phase space projections of the electronic distribution function. (a) Longitudinal momentum. (b) Transverse momentum along the direction of the laser electric field. (c) Transverse momentum along the direction of the laser magnetic field. In 2D simulations, the projections (a) and (b) are similar to the 3D case.

with the same parameters also exhibit bunched jets in the direction of the electric field with similar amplitude. As shown in [10] the electron bunches are responsible for OTS radiation at $2\omega_0$ at the rear of the target which suggests a ballistic propagation through it. The examination of the projection (p_y, p_z) averaged over few wavelengths in the longitudinal direction shows that the distribution function is isotropic, which confirms that the energy spread has a similar value in y and z . On a longer time scale the picture becomes more diffused with more and more heating of the bulk of the distribution function.

The observed transverse momentum spreading is a multidimensional effect, which does not occur in 1D, as observed in simulations [11]. In this case, the conservation of transverse momentum implies that no transverse velocity would persist when the energetic particles leave the skin depth, despite the existence of large transverse velocities in the skin depth layer. In 2D and 3D simulations, the energetic particle beam interacts with the dense plasma to generate magnetic fields oscillating in the transverse direction with very short wavelengths. The transverse momen-

tum invariance is broken and angular dispersion takes place. We have used the quasilinear theory to show that the transverse mean velocity in the laser electric field direction results from the coupling between the laser magnetic field and the Weibel instability inside the skin layer. In the following, the unit for momentum is mc , where m is the electron rest mass; the unit length and unit time are k_0^{-1} and $(k_0c)^{-1}$. The Weibel instability magnetic field is defined by $b(x, y) = \Sigma \beta(k, x) \exp(iky)$, with $(k_0c)m/e$ as the unit and assumed to be stationary for simplicity. Because the skin layer width is much smaller than the vacuum laser wavelength, particles with velocities close to the velocity of light travel across the skin layer in a time short enough to neglect the laser field time dependence. Consequently, if \mathbf{p} is the particle momentum, $\gamma = (1 + p^2)^{1/2}$ may be assumed to be constant during the motion. With the same units, the laser magnetic field is $B(x) = dA/dx$, where $A(x)$ is the y component of the vector magnetic potential. Inside the skin layer, B is larger than b so that a perturbation theory may be used to compute the transverse velocity v_y . At lowest order, b is neglected. At first order, out of the skin layer, the residual transverse velocity vanishes when averaged over the transverse coordinate y , but it determines the mean square angular scattering of particles. The second order provides a nonvanishing averaged transverse velocity Δv . For energetic particles normally incident at $x = 0$ on the plasma-vacuum interface, the mean square of the transverse velocity is given by $\langle v_y^2 \rangle = \gamma^{-2} \langle [\int_0^x dx' b(x', y')]^2 \rangle$, with $y' = y'(x') = y + \gamma^{-1} \int_0^x dx'' A(x'')$. The mean transverse velocity is given, with the same approximations by $\langle v_y \rangle = \gamma^{-1} A(x) + \Delta v$, where $\Delta v = \gamma^{-2} \sum_k \int_0^x dx' \int_0^{x'} dx'' \int_0^{x''} dx''' ik c_k(x''', x') \times \exp ik(y'' - y')$ is the second order mean particle transverse velocity with $y''' = y'(x''')$ and $c_k(x_1, x_2) = \langle \beta(k, x_1) \beta(-k, x_2) \rangle$. If there was no laser field, we would have $A(x) = 0$, $y''' - y' = 0$ and the statistical distribution of the field perturbations $b(x, y)$ would be symmetrical with respect to $+y/-y$. As a result, c_k would be real and $\Delta v = 0$. In presence of the laser field, the laser vector potential is finite inside the skin layer and these symmetries are broken. However, the fluctuating magnetic field results from the interaction of many fast electrons bunches with the skin layer. Since the vector potential has performed many oscillations during the build time of the magnetic field, we are allowed to consider that the field statistical properties keep their symmetry and that c_k remains real. Then, we have:

$$\Delta v = \gamma^{-2} \sum_k \int_0^x dx' \int_0^{x'} dx'' \int_0^{x''} dx''' k c_k(x''', x''') \times \sin\left(k\gamma^{-1} \int_{x'''}^{x'} d\xi A(\xi)\right).$$

For large x , $\langle v_y \rangle$ reduces to Δv which displays the oscillation which was noticed for the transverse mean velocity

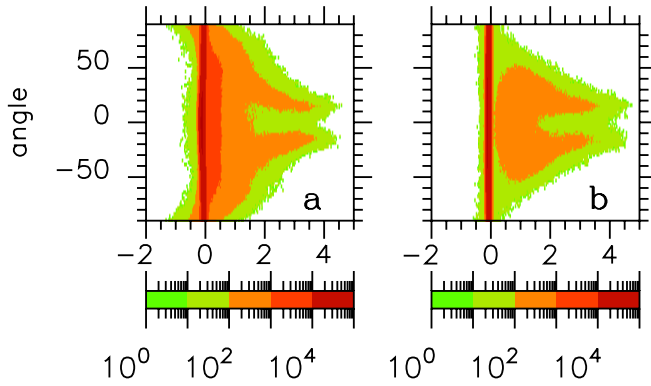


FIG. 4 (color online). Angular dispersion of the electrons in the 2D case. (a) Close to the interface, (b) approximately 2 laser wavelengths inside the plasma behind the maximum of the magnetic layer. Along the y axis, the angle of propagation of particles has been plotted in degrees; along the x axis the square root of the energy has been plotted with the sign corresponding to the direction of propagation along the longitudinal direction.

of the bunches. With these assumptions, the average transverse velocity changes its sign with A , in agreement with the simulation. The size of the observed mean velocity implies also that a large part of the beam deviation takes place mainly inside the magnetic layer. These equations also give the right order of magnitude both for the rms and the average value of the angular dispersion for high energy particles. To explain this concentration of the fluctuating magnetic field inside a thin layer close to the plasma-vacuum interface, it is necessary to look at the dispersion relation of the Weibel instability, taking into account both the hot particle beam and the return current. With weak velocity dispersions in the y and z direction, the instability growth rate peaks roughly at $\omega_{pe}(n_H/\gamma n_C)^{1/2}$ for $kd \geq 1$, where n_H and n_C are the beam and cold electron densities and d is the cold plasma skin depth. Inside a given hot electron bunch, the fast electron density is high enough to yield a large growth rate, allowing the instability to grow inside a thin layer close to the plasma-vacuum interface. But the short wavelength filamentation is rapidly stabilized by the transverse temperature increase. Modes remains unstable if $k^2 d^2 < (n_H/n_C)P_H^2/(\gamma\Delta^2)$, where P_H is the hot electron mean square longitudinal momentum and Δ is the rms hot electrons transverse momentum. Longer and longer wavelengths are excited with decreasing growth rates and saturation amplitudes. When the transverse momentum spread reaches the critical value such that $(n_H/n_C)P_H^2/(\gamma\Delta^2) = 1$, the modes are almost stabilized and only a residual weak instability survives at long wavelength.

In order to demonstrate that the magnetic field deflects the energetic particles we have developed a specific diagnostic that will be described in 2D. In a slab of given thickness and position, in the longitudinal direction, we “bin” the particles by energy range. For each energy range

we bin the particle according to their angle of propagation. Finally, we separate the particles with positive or negative values of v_x . The result is a 2D diagram that is shown in Fig. 4. It corresponds again to a 2D simulation with $n = 80n_C$, $\Phi = 10^{20}$ W/cm² and $T_e = 1$ keV. The plasma slab extends from $x = 100k_0^{-1}$ to $380k_0^{-1}$. Figure 4(a) is the spatial average taken between $105k_0^{-1}$ and $125k_0^{-1}$, 50 fs after the laser impact, this corresponds to a position slightly behind the magnetic layer. Figure 4(b) is a picture taken between $140k_0^{-1}$ and $160k_0^{-1}$ somewhat deeper in the plasma slab 70 fs after the laser impact. The time interval is such that it corresponds to the time it takes for the fastest particles to travel between the 2 slabs. This figure shows clearly that the particles are deflected by the magnetic layer and that they propagate then into the plasma without any further change of direction. One can also see that particles having abscissa larger than 1.5 (i.e., energy above 1 MeV) are, in this simulation, emitted in a cone with a half angle of approximately 20° . Later in time the cone tends to spread and to fill, yielding a much more diffuse picture with angles up to 30° or 40° . This corresponds to a further increase of the intensity of the magnetic field layer but also to an increase of its thickness.

As particles move away from the skin layer, reduction of the growth rate occurs due to the transverse temperature on a space scale equivalent to length necessary to spread them. Farther, particles propagate into the target with a quasi-static ballistic propagation.

In summary, we have performed 2D and 3D simulations that show that the divergence of energetic particles, observed in many experiments, is due to the development of a very thin and very intense filamented magnetic layer located in the vicinity of the laser-plasma interaction layer. The simulations yield divergence angles ranging between 20° and 40° in agreement with experiment results.

We are thankful to IDRIS (the CNRS computer center) for providing the computing resources necessary for this study.

-
- [1] A. Pukhov and J. Meyer ter Vehn, Phys. Rev. Lett. **79**, 2686 (1997).
 - [2] C. Ren *et al.*, Phys. Rev. Lett. **93**, 185004 (2004).
 - [3] R.J. Mason *et al.*, Phys. Rev. E **72**, 015401 (2005).
 - [4] Y. Sentoku *et al.*, Phys. Rev. E **65**, 046408 (2002), and references therein.
 - [5] H. Ruhl, Plasma Sources Sci. Technol. **11**, A154 (2002).
 - [6] F. Califano, D. Del Sarto, and F. Pegoraro, Phys. Rev. Lett. **96**, 105008 (2006).
 - [7] M. Tzoufras *et al.*, Phys. Rev. Lett. **96**, 105002 (2006).
 - [8] W.S. Lawson *et al.*, Phys. Plasmas **4**, 788 (1997).
 - [9] M. Honda *et al.*, Phys. Plasmas **7**, 1302 (2000).
 - [10] H. Popescu *et al.*, Phys. Plasmas **12**, 063106 (2005).
 - [11] W.L. Kruer and K. Estabrook, Phys. Fluids **28**, 430 (1985); S.C. Wilks *et al.*, Phys. Rev. Lett. **69**, 1383 (1992).